2014

Integration of Photovoltaics into Building Energy Usage through Advanced Control of Rooftop Unit

Michael Starke
Oak Ridge National Laboratory, United States of America, starkemr@ornl.gov

James Nutaro
Oak Ridge National Laboratory, United States of America, nutarojj@ornl.gov

Teja Kuruganti
Oak Ridge National Laboratory, United States of America, kurugantipv@ornl.gov

David Fugate
Oak Ridge National Laboratory, United States of America, fugatedl@ornl.gov

Integration of Photovoltaics into Building Energy Usage through Advanced Control of Rooftop Unit

Michael STARKE[1], James NUTARO[1], Philip IRMINGER[1], Ben OLLIS[1], Teja KURUGANTI[1], David FUGATE[1],

[1]Oak Ridge National Laboratory
1 Bethel Valley Road, Oak Ridge, TN, 37831
Email: starkemr@ornl.gov

ABSTRACT

This paper presents a computational approach to forecast photovoltaic (PV) power in kW based on a neural network linkage of publicly available cloud cover data and on-site solar irradiance sensor data. We also describe a control approach to utilize rooftop air conditioning units (RTUs) to support renewable integration. The PV forecasting method is validated using data from a rooftop PV panel installed on the Distributed Energy, Communications, and Controls (DECC) laboratory at Oak Ridge National Laboratory. The validation occurs in multiple phases to ensure that each component of the approach is the best representation of the actual expected output. The control of the RTU is based on model predictive methods.

1. INTRODUCTION

As the United States witnesses continued expansion of photovoltaic (PV) and other distributed generation technologies into the electric power grid and the retirement of traditional fossil fuel generation assets, there is an increased need to find approaches to mitigate integration challenges. The integration challenges vary by type of renewable resource but overall require more flexibility and support from other resources. These resources are appearing in the form of load side management, fast responding generation (natural gas) assets, and energy storage technologies [1].

One challenge for renewable integration is the potential for reverse power flow into the distribution system, or the condition when the generation resource output power exceeds the load. This condition is not of significant concern for low penetrations of PV, but could lead to issues with high penetration. Reverse power flow has the potential to not only cause electric power system issues (over voltage on distribution feeders, increases in dangerous short circuit currents, and desensitization of protection leading to potential breaches of protection coordination, and incorrect operation of equipment [2]) but also lead to additional cost to the utility through the net-metering initiatives [3]. Net-metering currently provides an economic incentive for customers to sell power back to utilities at greater rate than the avoided variable costs. Furthermore, studies examining this incentive and expected growth in California have found that the net load (difference between forecasted load and variable generation resources) could alter entirely from conventional load shapes into what is known as the 'Duck Curve.' With high penetrations of PV, the net-load curve could have the appearance of a 'belly' during mid-afternoon with a high arch at the end of the day representing the neck of a duck. This initiates a new challenge for conventional generation, as higher ramping rates will be needed to overcome the reduced PV output during late afternoon –early evening hours [4]. This challenge is likely to lead to further hikes in overall electricity cost as power system operators will have to deal with these short steep ramp rates, over-generation risks, and decreased frequency response.

One method for reducing this reverse power flow and the impact of the potential 'Duck Curve' is to utilize the power generation locally in the commercial building even when the load usage may not be optimum. As an example, heating ventilation and air conditioning (HVAC) systems could store thermal energy by pre-heating or pre-cooling a building during high PV production to reduce the chance and impact of reverse power flow. This method could also be supplemented to reduce potential peak demand charges by considering the PV and managing the available 'behind the meter' assets. However, in order to maximize the linkage between the load and renewable production, a method for forecasting the amount of renewable resource and optimizing available assets for resource utilization is needed. In this paper, a method for forecasting PV output is developed as a supplement for load control of a rooftop

air conditioner unit (RTU) using publicly available data. The forecasting method uses an approach to estimate solar irradiance and applies the irradiance into a PV model for output in kW. A model for predictive control approach is discussed to provide the appropriate control for peak management through the RTU while considering PV. Future work discussing the integration of this control and prediction onto a real test-bed is discussed.

2. PHOTOVOLTAIC GRID INTEGRATION USING LOAD AS A RESOURCE

2.1 PV Prediction

The overall approach utilized in this paper for forecasting the power output from a PV array is shown in Figure 1. The key elements to this approach are establishing the solar irradiance and the actual produced kilowatts (KW) from the PV panel. This is not a trivial solution, as the solar irradiance is governed by many factors including cloud cover, sun angle, and PV panel tilt. From the solar irradiance, the actual output power production is dependent on the specific PV panel manufacturer along with design and interface specification of power electronics (usually a standard inverter that converts the DC output generated by PV to AC). In this study, the objective is to forecast an hourly power production and utilize the energy as available from PV with future work looking into more dynamic control and use as shorter time interval forecasting is needed and requires further development. A Matlab based program has been created to collect the data and perform the necessary computation.

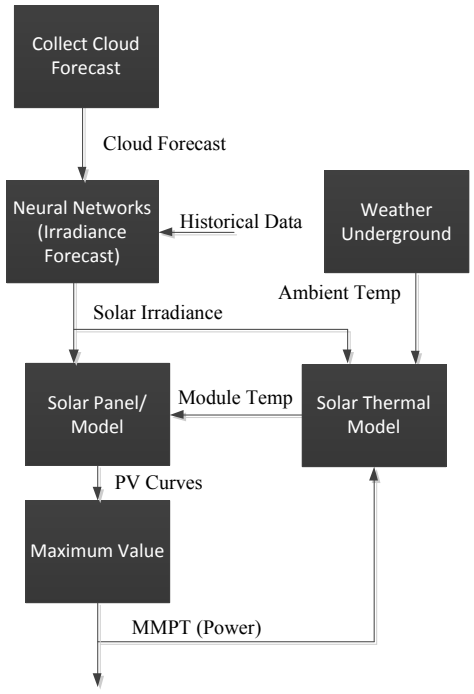

Figure 1: Overall approach to forecast PV output

Forecasting the solar irradiance collected by the PV panel requires data from a number of sources. Historical solar irradiance measurements, cloud patterns, and solar angles provide an important element to the ability to forecast the expected irradiance in an hourly time-scale. Figure 2 shows an example cloud cover for December 10th, 2013 for the eastern U.S as provided by the Government of Canada for astronomical purposes [5]. The '+' marks the approximate location of Knoxville/Oak Ridge, Tennessee where the PV array at the DECC lab is located and data is available for a forecast as far out as 48 hours. Other resources such as NOAA also provide data on cloud cover including the different cloud layers.

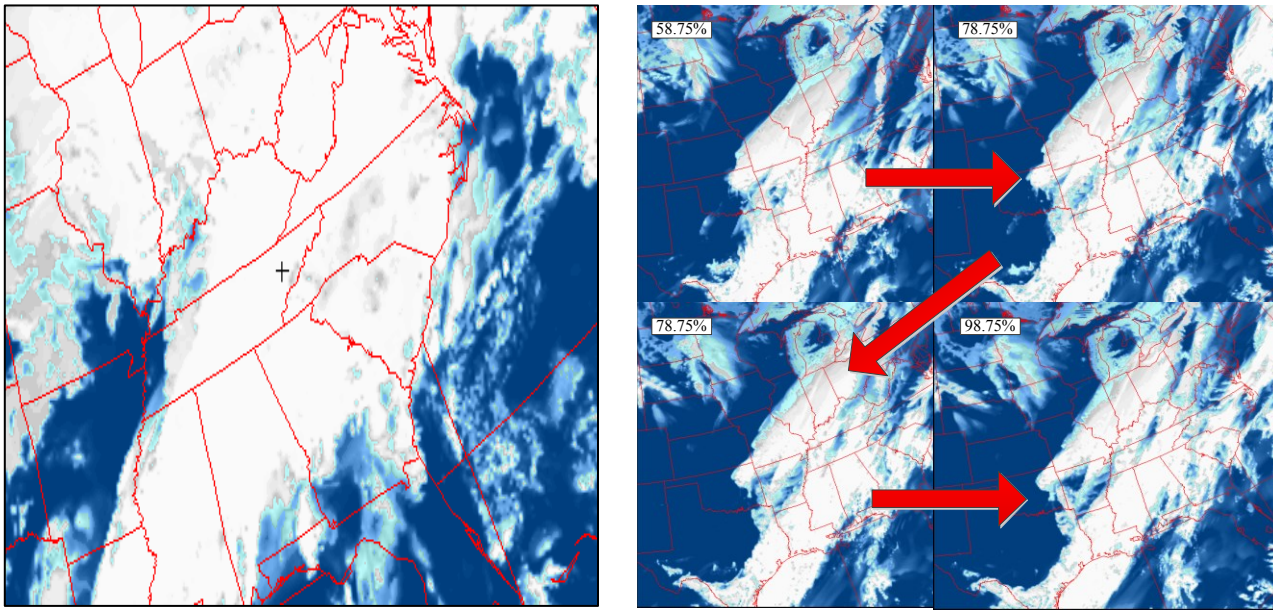

Figure 2: Example cloud cover for eastern U.S.

The cloud cover is identified by the color of the pixel on the map and can be found in a legend with the image source. During each hour, satellite forecast imagery is collected, the color for that coordinate extracted and the percent cloud cover determined as shown in Figure 2. This percent cloud cover is then inserted into a neural network algorithm along with zenith angle to find the relationship between the input data and measured solar irradiance. The zenith angle is determined using a separate Matlab code developed by Roy that utilizes the current time and GPS location of the which is available for download online [6-7]. For validating the results, the PV panel on the rooftop of the Distributed Energy, Communications, and Control (DECC) facility at Oak Ridge National Laboratory and the measured solar irradiance at this location are used. A picture of the installed PV is provided in Figure 3.

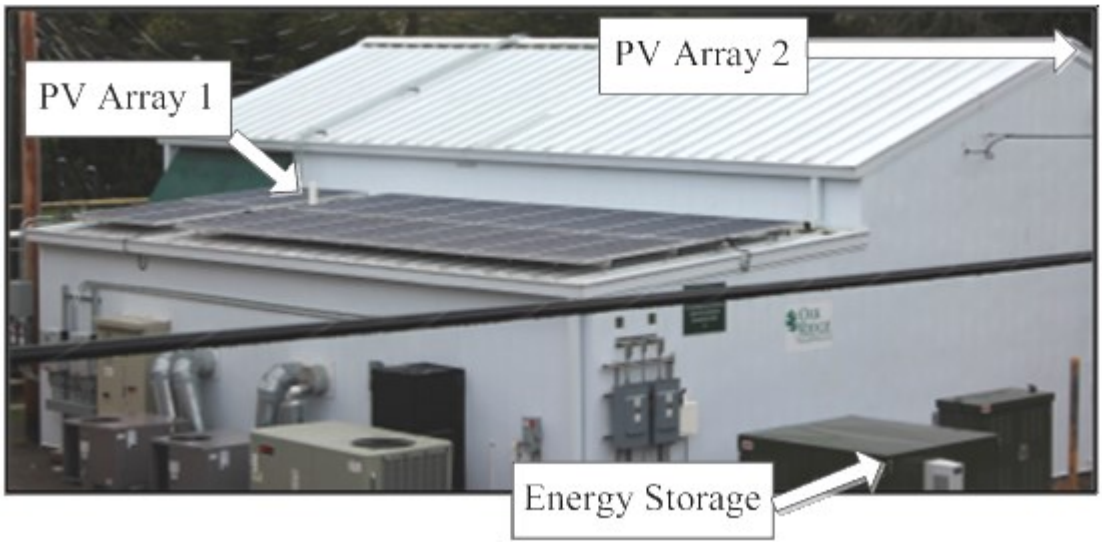

Figure 3: Picture of DECC laboratory and rooftop PV.

Significant literature is available on the modeling of PV cells and arrays. Many of these sources provide similar methods in modeling and capturing the PV characteristics. In this paper, the models developed by Villalva [8-9] are utilized in constructing the model due to the amount of required input details and the components considered. This model utilizes an input of solar irradiance and module temperature to estimate the output power based on an interconnected voltage.

In this method, the PV model is represented by a dependent current source with parallel diode, parallel resistance, and series resistance as shown in Figure 4. The output current of the PV module is a function of the current source minus the diode current and current passing through the parallel resistance R_p:

$$I = I_{pv} - I_o\left[e^{\left(\frac{(V+R_sI)}{V_t a}\right)} - 1\right] - \frac{(V+R_sI)}{R_p} \quad (1)$$

where I is the output current of the module, I_{pv} is the photovoltaic current, I_o is the diode saturation current, V_t is the thermal voltage, V the module voltage, R_s the series resistance, R_p the parallel resistance, a is the diode constant (typically in the range of 1 to 1.5).

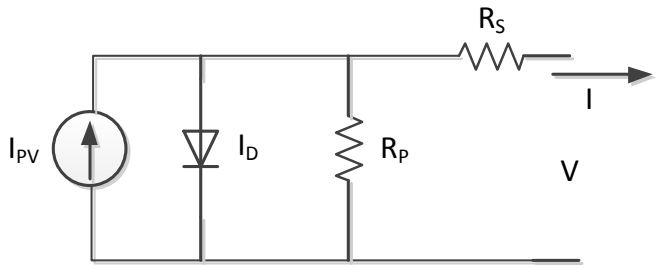

Figure 4: PV circuit representation

The thermal voltage is a characteristic given to diodes and can be calculated with

$$V_t = N_s kT/q \quad (2)$$

where N_s is the number of cells connected in series to produce the specific PV module, k is the Boltzmann constant, q is the electron charge and T is the temperature at the p-n junction or module temperature.

The photovoltaic current, or current source in Figure 4, is related to the collected solar irradiance and module temperature and is given by

$$I_{pv} = (I_{pvn} + K_I(T - T_n)\frac{G}{G_n} \quad (3)$$

where I_{pvn} is the light generated current at nominal conditions (which are specified by the manufacturer), K_I is the coefficient of the current in relation to temperature change, T-T_n is the difference in temperature from the measured and nominal temperature, G is the measured solar irradiance in W/m^2, and G_n is the solar irradiance at nominal conditions, usually 1000W/m^2.

The diode saturation current is also impacted by temperature and is given as

$$I_o = \frac{I_{scn} + K_I(T - T_n)}{e^{\left(\frac{(V_{ocn} + K_V(T - T_n)}{V_t a}\right)} - 1} \quad (4)$$

where I_{scn} is the short circuit current of the PV panel at nominal conditions, V_{ocn} is the open circuit voltage at nominal conditions, and K_v is the coefficient of the voltage in relation to the temperature change.

The resistance values R_p and R_s are calculated iteratively through the method described in [8-9] and are specific to a PV module and configuration. Equations 1-4 are applied along with the circuit model illustrated in Figure 4 to create the relationship between the output voltage and current, module temperature, and solar irradiance. The PV module model is incremented from 0 to the characteristic open circuit voltage of the PV system to create the current and power curves for the PV panel. At DECC, one of the strings of PV panels connected is composed of 12 modules in series and 2 sets in parallel. The resulting PV characteristic curves relating the developed voltage-current and power-voltage relationships are shown in Figure 5.

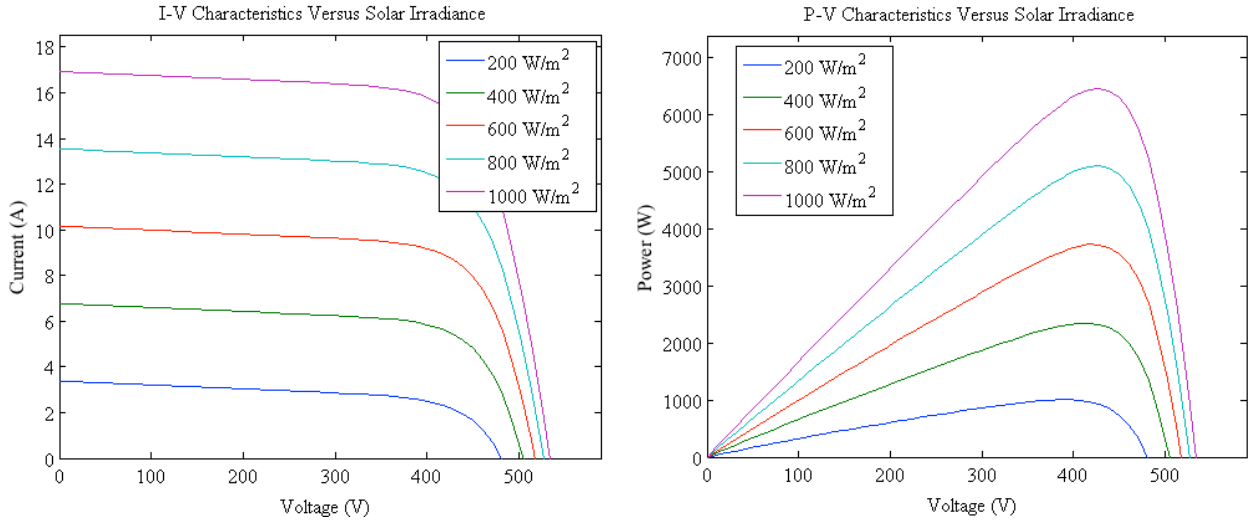

Figure 5: Characteristics for single PV array on DECC @25C

The circuit model and current source are controlled based on typical PV parameters that often can be located in a PV vendor datasheet. In this case, the module parameters for a 280W Hanwha Solar PV are used and are the same modules interconnected at the DECC facility. These are provided in Table 1.

Table 1: HSL72 Hanwha Solar PV Module Parameters [10]

Information	Number
Maximum Power (Pmax)	280 W
Voltage at MP (Vmp)	35.7 V
Current at MP (Imp)	7.84 A
Voltage Open Circuit (Voc)	44.6 V
Current at Short Circuit (Isc)	8.43 A
Ki	0.005058 A/K
Kv	-0.14718 V/K
Ns	72

In order to utilize the PV model developed by Villalva, the PV module temperature is a necessary component. The temperature on the module changes significantly during the day due to solar irradiance and outside temperatures. Jones provides a thermal module for a PV module that was developed to account for the increase and decrease in temperature of the modules [11]. The change in module temperature can be found by:

$$C_{module}\frac{dT}{dt} = q_{lw} + q_{sw} + q_{conv} - P_{out} \quad (5)$$

where C_{module} is the heat capacity of the module, q_{lw} is the long wave radiation heat transfer, q_{sw} is the short wave heat transfer, q_{conv} is the convection heat transfer, and P_{out} is the power generated by the module. The heat capacity of the module can be calculated with the basic information of the module:

$$C_{module} = \sum_m A d_m p_m C_m \quad (6)$$

where A is the area of the module, d_m is the depth of a specific layer, p_m is the density of the layer, and c_m is the specific heat of the layer. The equations for the short wave, long wave, convection heat transfer can be found in [11].

Today, in many cases, the interconnected PV inverter controls the PV DC link voltage such that the output of the PV is the maximum achievable power based on the solar irradiance (often termed maximum power point tracking-MPPT.) The PV curve developed based on measured solar irradiance at the given time is developed and the maximum power is extracted and assumed to be produced by the PV panel. This power is also reduced by a particular factor, which is associated with the efficiency of the interconnected inverter. In many cases, the efficiency performance in relationship to output power of the inverter is available from the manufacturer.

2.2 PV Model Validation Results

In order to validate the modeling and forecasting approach, validation is conducted at different steps of the development of the PV power output. First, the real irradiance measurement on the PV panels, archived on a 15 minute average through the PV monitoring system, is compared with the estimated irradiance from the model. In this example case, the week of 4/6/2014 - 4/12/2014 is examined utilizing training from the previous 3 months. Figure 6 shows the direct comparison comparison. The results demonstrate that the measured versus solar irradiance overall consistently match the measured irradiance. The only outlier is the 6th day. This is believed to be a result of a mis-forecast on cloud cover. As seen in Figure 7, there is predicted to be a high percentage of cloud cover for the 6th day, however the measured irradiance appears to see no difference compared to the previous clear day.

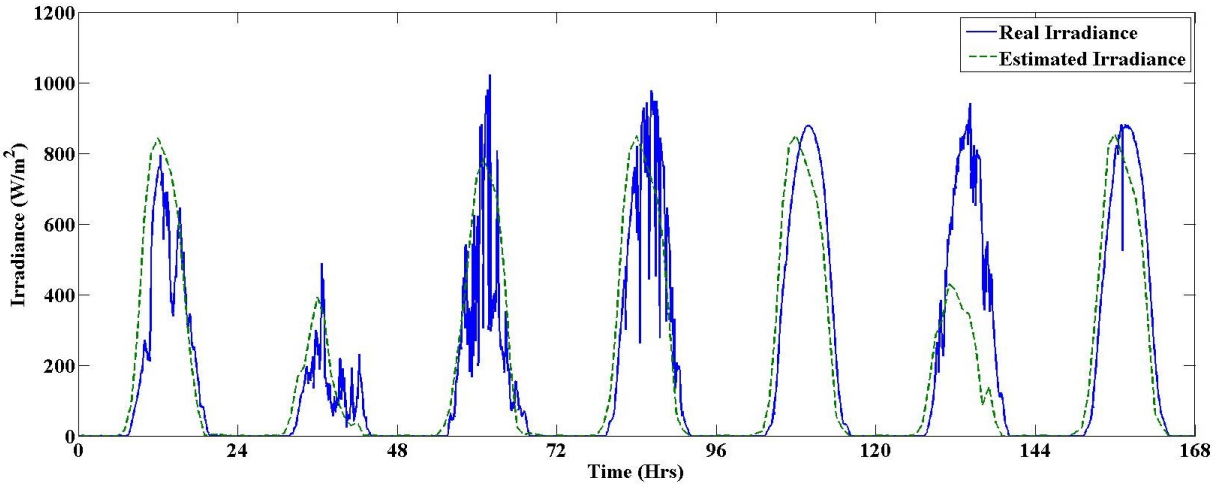

Figure 6: Comparison of estimated irradiance and real irradiance measurements

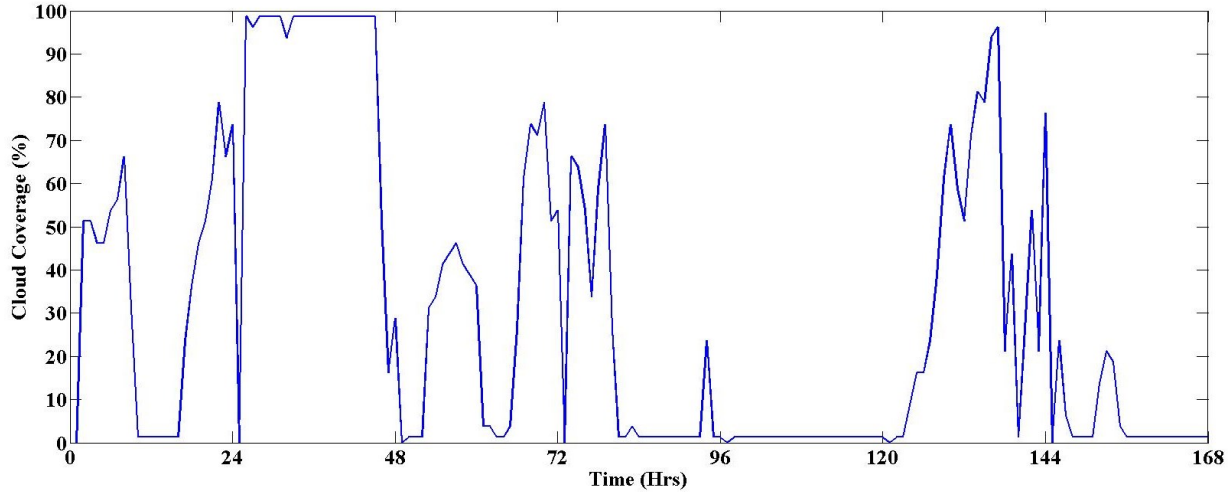

Figure 7: Estimated cloud cover from image analysis

A second component to the validation involved the modeling of the temperature rise of the PV panel. As previously mentioned, the temperature is impacted by both the heating from solar irradiance and the outside ambient temperature. These measured inputs along with the kW from the PV panel are inserted into the model and the output of the module temperature is recorded. The results from this comparison can be seen in Figure 8. This test was constructed to run all seven days consecutively and as a result error can propagate as shown. Even with seven consecutive days, only a 10K difference in temperature is seen during peak hours. This will lead to a small percentage of overall error in the full model. Furthermore, the parameters for the PV thermal model could be better tuned to specifically match this PV panel.

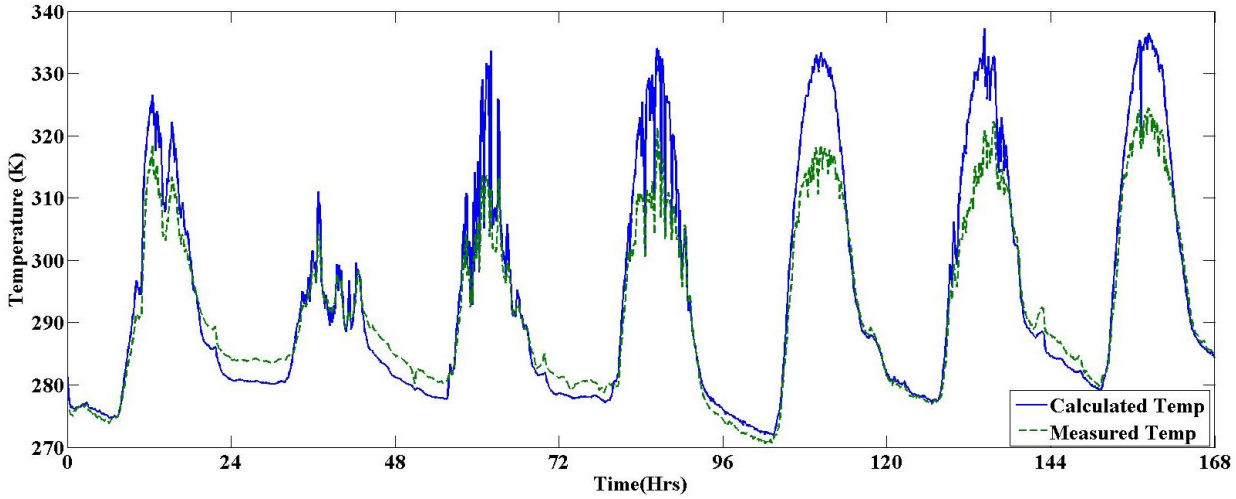

Figure 8: Comparison of calculated PV module temperatures and measured module temperatures

The third step in validation involved the PV model with inputs of solar irradiance and module temperature and output of power. Here the measured quantities of solar irradiance and module temperature are inserted as inputs and used to compare the measured and actual power output of the PV considering MPPT. The results from this comparison can be seen in Figure 9. As seen the output measured PV power and modeled PV power are highly correlated.

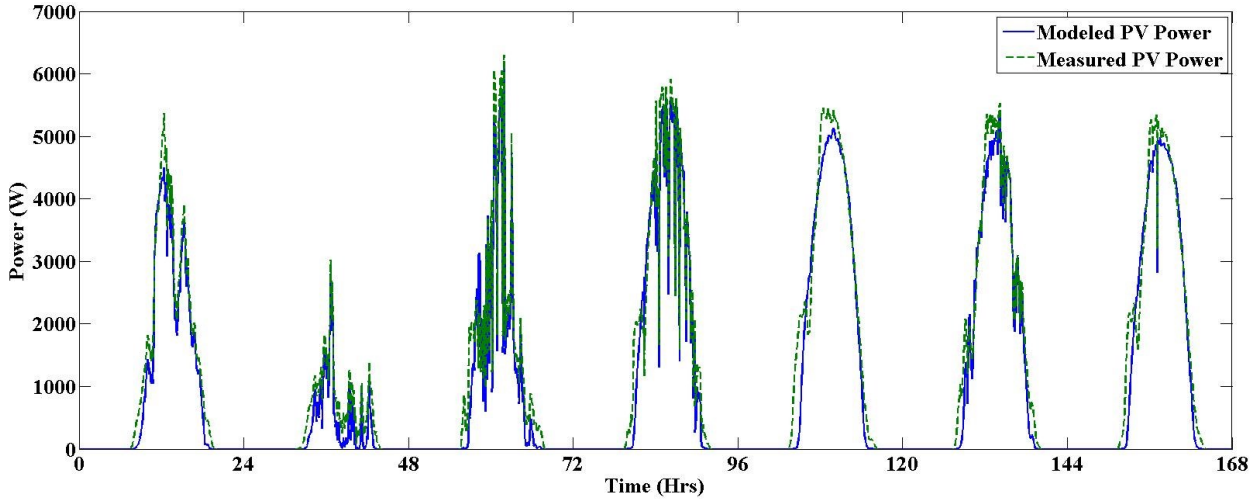

Figure 9: Comparison of modeled power output utilizing real module temperatures and measured irradiance measurements

The fourth and final validation involved interlinking all of the calculation components and performing a full forecast while using no measured data. The results from this analysis is shown in Figure 10. In Figure 10, the forecasted output PV power and measured power are compared. The root mean square (RMS) range for the period considering each day separately is 368 to 1538W with an average RMS error of 813W. The average error range for the power per day range is -31W to -837W with a total average -164W for the week. The solar irradiance error range in RMS is 65.96W/m^2 to 229W/m^2 with an average of RMS error of 132W/m^2.

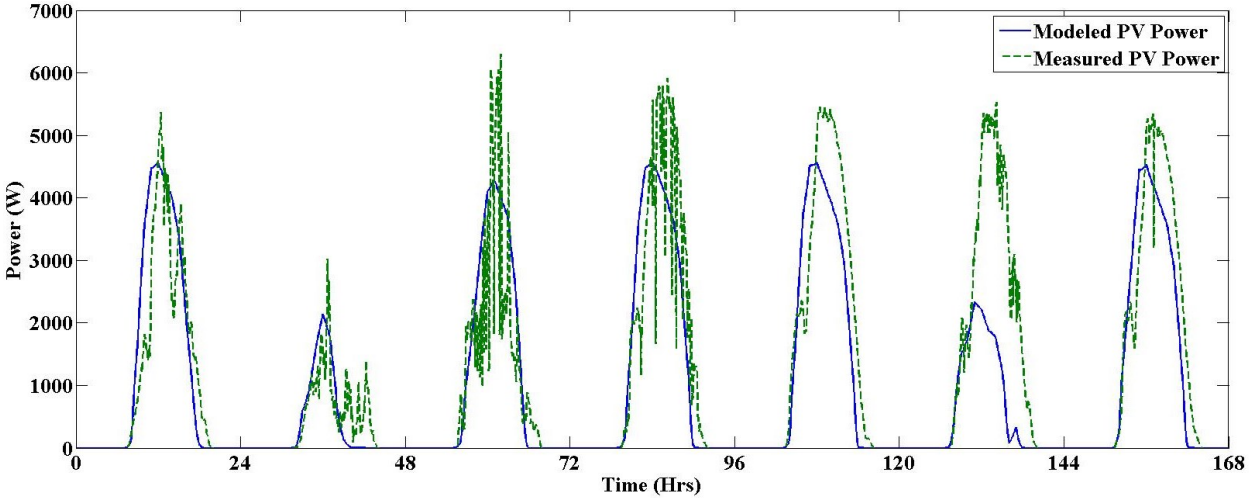

Figure 10: Comparison of modeled power output utilizing predictions against the measured power output

2.3 Optimization and Objective

In related work [12], we have proposed a model predicative control that seeks to maintain satisfactory comfort for the building occupants while reducing peak power consumption by the air conditioning units. This is accomplished by simultaneously operating no more than N air conditioning units when a total of $M > N$ units are available. The assumption is that each air conditioning unit is responsible for heating and cooling a particular space, or zone, within

the building, and for this purpose each air conditioning unit k is connected to a thermostat that measures the air temperature T_k, has a reference temperature $T_{ref,k}$, and has dead bands $\Delta T_{c,k}$ and $\Delta T_{h,k}$.

The model predicative control divides time into control periods of p minutes, and at the beginning of each period it selects which units to operate. The selection process has two phases. In the first phase, the control decides which units are eligible for activation. A unit is eligible to cool if the temperature $T_k > T_{ref,k} + \Delta T_{c,k}$ and to heat if $T_k < T_{ref,k} - \Delta T_{h,k}$. In the second phase, the control selects which eligible units to activate. This selection comprises at most N of the eligible units picked such that the largest number of temperatures T_k will be within their desired range at the end of the control period. This is accomplished with a model that predicts the temperature T_k' at the end of the control period and choosing the fewest eligible units N^* that minimize the expression

$$T^* = \sum_k \max\left\{T_k' - \left(T_{ref,k} + \Delta T_{c,k}\right), 0\right\} + \max\left\{\left(T_{ref,k} - \Delta T_{h,k}\right) - T_k', 0\right\} \tag{7}$$

Given information about the availability of PV power over the next control period, this control can be augmented so that it prefers to operate the air conditioning units when PV power is available. Given the power consumption P of an HVAC unit and the forecasted power P_{solar}, the amount of power that must be drawn from the grid (rather than the PV) is given by

$$P^* = \max\{PN^* - P_{solar}, 0\} \tag{8}$$

The terms T^* and P^* are weighted according to the preference for controlling temperature versus using electrical power from the solar panel to obtain an objective function

$$w_1 T^* + w_2 P^* \tag{9}$$

Table 1 demonstrates the trade between the error in the temperature control and the mean rate of power drawn from the electrical grid as the weights w_1 and $w_2 = 1 - w_1$ are varied. The data in Table 1 is notional, being based on a simulation study of a four zone building similar to the one described in [12] with the individual zones and solar irradiance modeled as described in [13], but it illustrates how an effective PV forecast can be used to reduce energy consumption with a modest reduction in the ability to regulate temperature. The table shows mean values of P^* and T^* over five simulated days assuming an idealized forecast for P_{solar} over the next control period. The outdoor air temperature was selected to mimic a spring day in Knoxville, TN and ranged from a nighttime low of 15 deg. C and daytime high of 30 deg. C. The temperature band for the control was from 24 to 25 deg. C.

Table 1: Control error versus power consumption.

w_1	Mean P^* (kW)	Mean T^* (deg. C)
1	0.537	0.0652
0.95	0.0839	0.158
0.9	0.0286	0.174
0.85	0.0237	0.175
0.8	0.0133	0.182
0.75	0.00929	0.184
0.7	0.00515	0.187
0.65	0.00212	0.189
0.6	0.00171	0.190

3. CONCLUSIONS AND FUTURE WORK

This paper discusses a computational approach to forecast PV power in kW, 24 hours ahead, based on a neural network linkage of publicly available cloud cover snapshots and collected solar irradiance data and PV models and mentions a control approach to utilize rooftop air conditioning units (RTUs) to support renewable integration. The PV forecasting method is validated through examining a rooftop PV panel installed on the Distributed Energy,

Communications, and Controls laboratory at Oak Ridge National Laboratory. The validation occurs in multi-phases to ensure that each component of the approach is the best representation of the actual expected output. The control of the RTU is based on model predictive methods.

Future work will continue to consider and adapt the PV forecasting to consider more data and potentially shorter time-window forecasts as other methods are included. Resolution of the cloud cover from the snapshots is very low and often captures the general cloud behaviors but does not provide accuracy on when cloud cover transients will occur. Future updates will be incorporated to improve this resolution. The control will also be implemented into RTUs located at the flexible research platforms at ORNL. This will provide real data on control development and testing of the RTUs in respect to PV output power.

REFERENCES

[1] L. Bird, M. Milligan, D. Lew, "Integrating Variable Renewable Energy: Challenges and Solutions," NREL/TP-6A20-60451, September 2013.

[2] E. Liu, J. Bebic, "Distribution System Voltage Performance Analysis for High-Penetration Photovoltaics," NREL/SR-581-42298, February 2008.

[3] P. Kind, "Disruptive Challenges: Financial Implications and Strategic Responses to a Changing Retail Electric Business," Edison Electric Institute, January 2013. Available online at: http://www.eei.org/ourissues/finance/documents/disruptivechallenges.pdf

[4] California ISO, "What the duck curve tells us about managing a green grid," Available online at http://www.caiso.com/Documents/FlexibleResourcesHelpRenewables_FastFacts.pdf

[5] Government of Canada, Clouds Forecast for Astronomical Purpose, Available online at: http://weather.gc.ca/astro/clds_vis_e.html

[6] V. Roy, Sun Position, available online at: http://www.mathworks.com/matlabcentral/fileexchange/4605-sunposition-m

[7] I. Reda, A. Andreas, "Solar Position Algorithm for Solar Radiation Applications," NREL/TP-560-34302, January 2008.

[8] M.G. Villalva, J.R. Gazoli, E.R. Filho, "Modeling and circuit-based simulation of photovoltaic arrays," Brazilian Power Electronics Conference (COBEP '09) , pp. 1244-1254, Sept. 27 2009-Oct. 1 2009.

[9] M.G. Villalva, J.R. Gazoli, E.R. Filho, "Comprehensive Approach to Modeling and Simulation of Photovoltaic Arrays," IEEE Transactions on Power Electronics, vol. 24, no. 5, pp. 1198-1208, May 2009.

[10] Hanwha Solar, Datasheet for HSL 72 Hanwaho Solar Module, available online at: http://www.civicsolar.com/sites/default/files/documents/hsl72poly-103170.pdf

[11] A.D. Jones, C.P. Underwood, "A thermal model for photovoltaic systems", Solar Energy, Vol. 70, Issue 4, 2001, pp. 349-359, http://dx.doi.org/10.1016/S0038-092X(00)00149-3.

[12] J. Nutaro, D. Fugate, T. Kuruganti, M. Starke, "An inexpensive retrofit technology for reducing peak power demand in small and medium commercial buildings", Proceedings of the 3rd International High Performance Buildings Conference at Purdue, July 14-17, 2014.

[13] R. Gondhalekar, F. Oldewurtel and C.N. Jones, "Least-restrictive robust MPC of periodic affine systems with application to building climate control", 49th IEEE Conference on Decision and Control (CDC), pp. 5257-5263, 2010.

ACKNOWLEDGEMENT

This paper has been authored by employees of UT-Battelle, LLC, under contract DE-AC05-00OR22725 with the U.S. Department of Energy. Accordingly, the United States Government retains and the publisher, by accepting the article for publication, acknowledges that the United States Government retains a non-exclusive, paid-up, irrevocable, world-wide license to publish or reproduce the published form of this manuscript, or allow others to do so, for United States Government purposes.